# Production of $C_3/C_4$ Olefins from *n*-Hexane: Conceptual Design of a Catalytic Oxidative Cracking Process and Comparison to Steam Cracking

**C. Boyadjian,*,† K. Seshan,† L. Lefferts,† A. G. J. van der Ham,‡ and H. van den Berg§**

*Catalytic Processes & Materials, Membrane Technology, and Process Plant Design, Faculty of Science & Technology, University of Twente, IMPACT, P.O. Box 217, 7500 AE, Enschede, The Netherlands*

A conceptual design of the catalytic oxidative cracking (COC) of hexane as a model compound of naphtha is reported. The design is based on experimental data which are elaborated through a structural design method to a process flow sheet. The potential of COC as an alternative to steam cracking (SC) is discussed through comparing the key differences between the two processes. The presence of Li/MgO catalyst in the COC process (i) induces hexane cracking at lower operation temperatures (575 °C) than in SC (800 °C) and (ii) controls the olefin distribution by increasing the ratio of (butylene + propylene)/ethylene. The product distribution, and thus the separation train of both processes, is different. Catalytic oxidative cracking is designed to maximize propylene and butylene production, while steam cracking is designed to maximize ethylene production. In comparison to SC, the COC process is more energy efficient and consumes 53% less total duty for a production capacity of 300 kton/year of light olefins. However, a preliminary economic evaluation illustrates that the loss of valuable feedstock as a result of combustion of part of the naphtha feed makes the COC process economically less attractive than SC.

## 1. Introduction

Light olefins (ethylene ($C_2^=$), propylene ($C_3^=$), and butylenes ($C_4^=$)) are the building blocks for the chemical industry. They are currently the raw materials for the synthesis of (i) bulk chemicals, e.g., ethylene oxide and acrolein; (ii) polymers, e.g., polyethylene, -propylene, or -butylenes; and (iii) fuels such as diesel and gasoline, e.g., by butene/butane alkylation. In a world with continuous development in the production of new synthetic materials, the demand for these petrochemicals is increasing tremendously, and a growth rate of 4% is predicted for the coming years.[1] The propylene market is growing faster than the ethylene market by ∼1%.[1] Thus, propylene yields from current production technologies are unlikely to be able to satisfy these demands.

Steam cracking (SC), despite being the major route for the production of light olefins, is less attractive both environmentally and economically, as it is the most energy-consuming process in the chemical industry. It is reported[1] that the pyrolysis section of a naphtha steam cracker alone consumes approximately 65% of the total process energy required and generates approximately 75% of the total exergy loss. Moreover, the process is accompanied by high emissions of $CO_2$ as a result of fuel combustion. The drawbacks of this process have urged substantial interest in the development of alternative routes for light olefin production.[1] Although intensive research is performed in this area, only a few processes have been commercialized. Catalytic dehydrogenation processes (Oleflex, STAR, FDB-4, Catofin) were developed in the early 1980s as alternative routes for light olefin production.[2−4] However, these processes have made only limited breakthroughs commercially. The major disadvantages of this route is the thermodynamic equilibrium, leading to limited yields, and the strong tendency to coking and consequently catalyst deactivation, leading to short lifetimes of the catalyst.

Catalytic oxidative cracking (COC) of naphtha to light olefins is conceptually a promising alternative to SC for a variety of reasons: (i) the process runs autothermally—reaction in the presence of oxygen is exothermic, and therefore the energy required for cracking can be generated *in situ*; (ii) the presence of oxygen shifts the thermodynamic equilibrium, overcoming the olefin yield limitations encountered during the dehydrogenation reactions; and (iii) the presence of oxygen limits the extent of coking. Moreover, the presence of a catalyst enhances the C−H and C−C bond cleavage in the alkane, thus inducing activity at lower temperatures than those utilized in SC. We expect that with oxygen cofeeding (autothermal operation) and catalytically induced reaction at relatively low temperatures, the external energy input (fuel combustion) will be minimized, and consequently $CO_x$ and $NO_x$ emissions will be reduced. Moreover, with the presence of a catalyst, we aim to control the olefin distribution by increasing the ratio of the high olefins (propylene, butylenes) to ethylene. This is possible to some extent in SC by varying reaction conditions; nevertheless, ethylene remains the major product.[1]

The development of an efficient oxidation catalyst that minimizes combustion, however, remains a challenge. The right catalyst should be able to selectively activate the alkane in the presence of the very reactive olefins, thus inhibiting the consecutive deep oxidation of the product olefins. Li/MgO catalyst has shown promising performance for the oxidative dehydrogenation/cracking of light alkanes[5−14] and recently for the oxidative cracking of hexane.[15] Li/MgO is basic in nature and possesses no formal redox properties. Therefore, unlike the case in oxidic catalysts with redox properties, e.g., $V_2O_5/MgO$,[16] consecutive combustion of olefins over this catalyst is significantly suppressed. Thus, the high selectivities to olefins are maintained, even at high alkane conversions.[12−15] In the oxidative cracking of butane and propane over Li/MgO catalyst, despite the high conversion levels achieved (70 mol % of *n*-butane and 60 mol % of propane), appreciable selectivities to light olefins of ∼60 mol % were obtained.[12]

In the present study, the technical feasibility of the COC process using hexane as a model compound for naphtha over

* To whom correspondence should be addressed. Tel.: +31-50-363 4826. Fax: +31-50-363 4479. E-mail: cassia.boyadjian@gmail.com.
† Catalytic Processes & Materials.
‡ Membrane Technology.
§ Process Plant Design.

10.1021/ie101432r 
Published on Web 11/19/2010

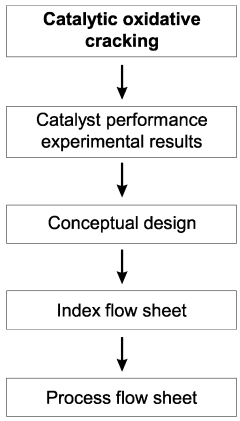


**Figure 1.** Steps to systematically create a process flow sheet.

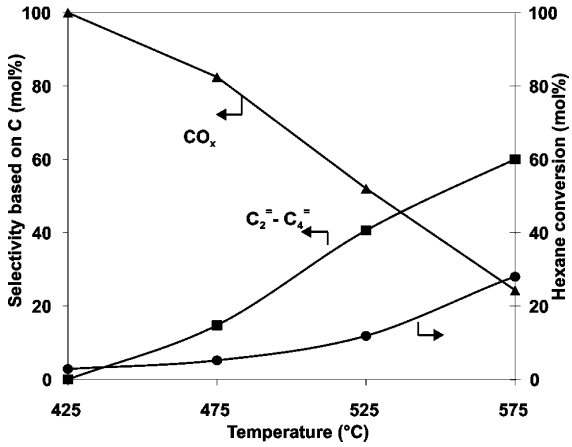


**Figure 2.** Influence of temperature on hexane conversions and selectivities to products during the oxidative cracking of hexane over Li/MgO. Reaction conditions: 100 mL/min; 10% hexane, 8% oxygen, balance helium; catalyst amount, 100 mg.[15]

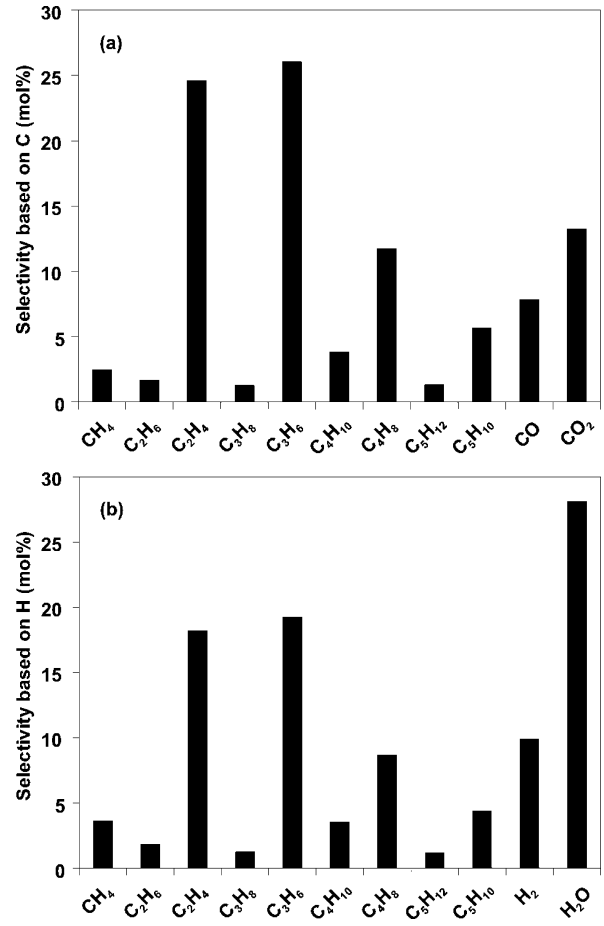


**Figure 3.** Product distribution observed during the oxidative cracking of hexane. Selectivities based on C (a) and based on H (b) are presented. Reaction conditions: 100 mL/min; 10% hexane, 8% oxygen, balance helium; $T = 575$ °C; catalyst amount, 300 mg; hexane conversion, 45 mol %.[15]

Li/MgO catalyst is reported. Moreover, the technical and economic potential of the process in comparison to SC is discussed. Experimental results from the oxidative cracking of hexane over Li/MgO catalyst previously reported by us[15] are the basis for the mass balance and design calculations. These results are utilized together with a structural design method[17,18] to develop, step-by-step, the process flow sheet for the oxidative cracking process (Figure 1).

## 2. Experimental Results

Experimental results of COC of hexane over Li/MgO are presented in Figures 2−4. The catalytic tests were carried out at atmospheric pressure and isothermal conditions in a conventional fixed-bed reactor. Total feed of 100 mL/min was used. The feed consisted of 10 mol % of hexane vapor, 8 mol % of $O_2$, and balance helium. Different hexane conversions were achieved by varying the weight hourly space velocity between 5 and 15.4 $h^{-1}$. The kinetic experimental setup and a detailed analysis of experimental results are reported in ref 15.

Results of experiments in the temperature range 425−575 °C (Figure 2) showed a clear influence of temperature on both hexane conversions and selectivity to products.[15] Hexane conversion increased with temperature. Gas-phase activation of hexane (not shown here) started to be noticeable at temperatures above 600 °C. Therefore, to minimize gas-phase non catalytic conversion of hexane, 575 °C was selected as an optimum temperature. It is generally believed that $[Li^+O^-]$ in Li/MgO is responsible for the catalytic activity. The $[O^-]$ site is a strong hydrogen abstractor and induces homolytic scission of the C−H bond in the hexane, forming a radical (eq 1).

$$C_6H_{14} + O^-{}_s \rightarrow C_6H_{13}^{\bullet} + OH^-{}_s \quad (1)$$

$$C_6H_{13}^{\bullet} + O_2(g) \rightarrow \alpha\text{-}C_1\text{−}C_5 \text{ (alkanes, olefins)} + \beta CO_x + \gamma H_2O + \delta H_2 \quad (2)$$

The formed radical then undergoes complex radical chemistry in the presence of oxygen in the gas phase (eq 2), forming a product mixture of $C_2$−$C_5$ olefins and $C_1$−$C_5$ alkanes, as well as combustion products ($H_2O$ and $CO_x$) and byproduct $H_2$.[15] Thus, oxidative cracking over Li/MgO is a heterogeneously initiated homogeneous reaction. With increasing temperature, a continuous decrease in $CO_x$ formation and a continuous increase in $C_2$−$C_4$ olefin formation was observed (Figure 2). A typical product mixture of COC over Li/MgO at 575 °C is given in Figure 3. At these reaction conditions (300 mg of catalyst), 45 mol % hexane conversion and 63 mol % selectivity (based on C) to $C_2$−$C_4$ olefins was observed. Carbon and hydrogen balance closed within ±5%.

Further, the influence of the mole fraction of oxygen in the feed on both hexane conversions and selectivities to olefins has been studied (Figure 4). Oxygen in the feed up to 4 mol % has a significant influence on hexane conversions. This is mainly explained by the role of oxygen in regenerating the catalyst by removing hydrogen from the surface $[Li^+OH^-]$ species (eq 3)

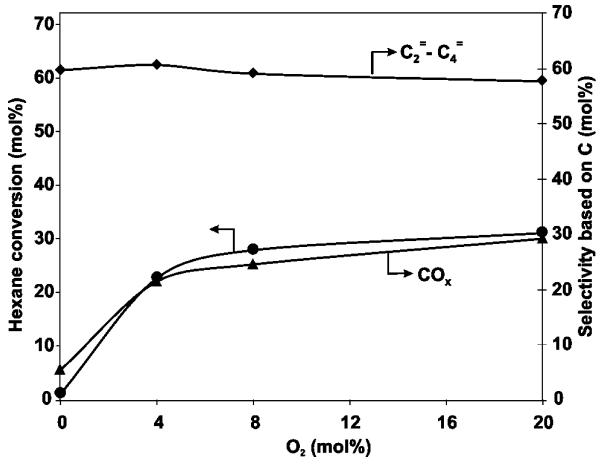


**Figure 4.** Influence of the mole fraction of oxygen on hexane conversion as well as selectivity to products: (●) hexane conversion, (▲) selectivity to $CO_x$, and (◆) selectivity to light olefins ($C_2^=-C_4^=$). Oxygen conversions: 68.5, 65.2, and 38.5 mol % at 4, 8, and 20 mol % $O_2$, respectively. Reaction conditions: 100 mL/min; 10% hexane and balance He; $T = 575$ °C; catalyst amount, 100 mg.[15]

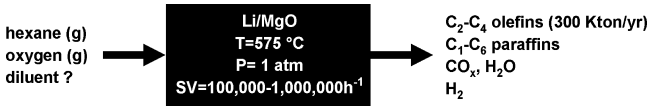


**Figure 5.** Black box of the COC process.

formed during the oxidation of hexane. The further slight increase in hexane conversion with increasing mole fraction of oxygen above 4 mol % is explained by the role of oxygen in accelerating the radical chemistry through the formation of $HO_2^\bullet$ radicals, which act as chain propagators in gas-phase reactions (eq 4). Oxygen also plays a significant role in inhibiting coke formation. However, increasing the mole fraction of oxygen results in an increase in $CO_x$ formation. Moreover, an increase in the risk of explosion is expected. Therefore, optimal oxygen mole fractions are necessary to maximize hexane conversions and minimize both combustion reactions and explosion risk.

$$2Li^+OH^- + {}^1/_2O_2 \rightarrow 2Li^+O^- + H_2O \quad (3)$$

$$C_nH_{2n+1}^\bullet + O_2 \rightarrow C_nH_{2n} + HO_2^\bullet \quad (4)$$

The reported experimental data of catalyst activity (45 mol % of hexane conversion) and selectivity to various products presented in Figure 3 are further utilized to determine the composition of feed and product streams of the process overall; hence, they are the basis for the mass balance and design calculations. However, it is necessary to note that these catalytic experiments were performed under conditions far from those to be implemented in a real process, where naphtha will be cracked at conditions set to maximize conversions. In these experiments, hexane was used as a model compound of naphtha. This is not unusual, as hexane cracking has been used to model naphtha cracking in fluid catalytic cracking (FCC) processes.[19] Moreover, in the experimental work our objective was to study the performance of the catalyst; hence, to minimize gas-phase activation of hexane, low mole fractions of hexane and oxygen were used by dilution in helium. The hexane-to-oxygen ratio to be used in this process design and choices regarding the dilution are discussed below in the conceptual design section. Figure 5 presents a black box of the process, identifying the key process overall parameters.

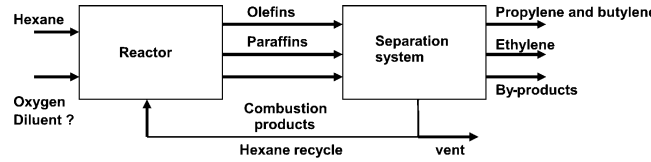


**Figure 6.** Functional block diagram of the COC process.

| Variable | Alternative 1 | Alternative 2 | Alternative 3 |
|---|---|---|---|
| Feed | Naphtha +air | Naphtha + $O_2$ + diluent | **Naphtha + $O_2$** |
| Reactor | Fixed bed reactor | **Fluidized bed reactor** | Catalytic membrane reactor |
| Separations | | | |
| $C_2^=/C_2$ | Absorption | **distillation** | membranes |
| $C_3^=/C_3$ | Pressure swing adsorption (PSA) | **distillation** | membranes |
| $C_4^=/C_4$ | OLEX process | **distillation** | membranes |
| Separation order | $C_2/C_3$ first | **$C_4/C_3$ first** | |
| Hydrogen | **Sell hydrogen as product** | Use hydrogen | |
| Heavies removal | With phase separators | **With distillation** | |

**Figure 7.** Alternatives and choices.

## 3. Conceptual Design

Figure 6 presents a functional block diagram of the COC process. The process feed consists of hexane and oxygen. The possible use of diluent is discussed later. Due to the low conversion in the reactor (45 mol %), it is decided to recycle the unconverted hexane. Propylene and butylenes are the main desired products and are recovered together and separately from ethylene and the remaining byproduct (heavy olefins ($C_5$), $C_1-C_5$ alkanes, $H_2$, $H_2O$, $CO_x$). Based on various process alternatives and choices, this block diagram is elaborated further to a comprehensive flow sheet. Overall process alternatives and choices made are given in Figure 7. Decisions and choices are further discussed below.

**3.1. Feed.** Hexane and oxygen are the only feeds to the process. Pure oxygen is decided to be utilized instead of air or a mixture of oxygen and diluent since the separation of the diluent (e.g., air or $N_2$) is complicated and costly. Thus, oxygen is considered as a commodity chemical which is purchased, hence avoiding the need for an air separation unit in the process. To avoid explosion, oxygen mole fractions in the reactor should be limited. Figure 8 presents the ternary diagram of explosion limits for a mixture of octane (as model compound of naphtha), oxygen, and hydrogen at reaction conditions. Since the reactor volume consists mainly of a mixture of hydrocarbons, oxygen, and hydrogen, the process should be operated at a very high volume percentage of alkane and a low volume percentage of oxygen to avoid explosive mixtures. Since one of the concepts of COC is autothermal operation, a certain amount of oxygen is required for the combustion of a part of the alkane feed. The minimum oxygen mole fraction required for autothermal operation was estimated using eqs 5−7 and was based on octane as the alkane feed. It is assumed that this estimation is also valid when hexane or naphtha is used as a feed. The relative reaction

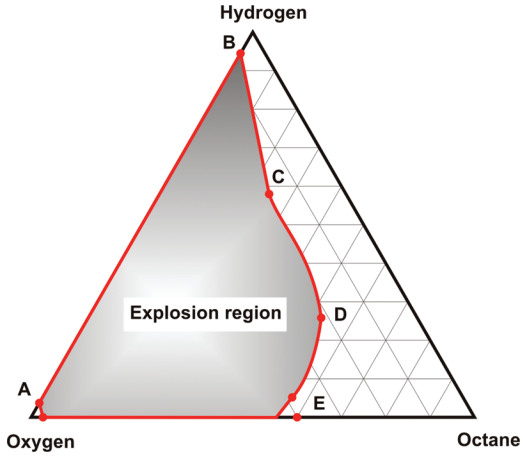


**Figure 8.** Explosion limits of reaction mixture at reaction conditions.[20]

**Table 1. Physical Properties of Octane**

| property | value |
|---|---|
| $C_{p,gas}$ (J/mol·K) | 241 |
| $C_{p,liquid}$ (J/mol·K) | 255 |
| $T_{boil}$ (K) | 399 |
| $\Delta H_{vap}$ (kJ/mol·K) | 35 |
| HHV (kJ/mol) | 5074 |
| HHV (kJ/kg) | 44419 |
| $\Delta H_{reaction}$ (kJ/mol) | 416 |
| $T_{reaction}$ (K) | 775 |

enthalpies of eqs 6and 7 are almost invariant with the carbon number; i.e., $\Delta H_r/\Delta H_{comb} = 0.082$ and 0.078 for octane and hexane, respectively.

$$f_{burned} - \Delta H_{combustion} = (1 - f_{burned})(\Delta H_{vap} + \underset{[evaporation]}{} C_{p,liquid}(T_{boil} - T_{feed}) + C_{p,gas}(T_{reaction} - T_{boil}) + \zeta\Delta H_r) \quad (5)$$
$$[liquid\ heating] \qquad [gas\ heating] \qquad [heat\ of\ reaction]$$

The values of the required parameters are given in Table 1. It is assumed that the uncombusted octane reacts to four molecules of ethylene and one molecule of hydrogen (eq 6).

$$C_8H_{18} \rightarrow 4C_2H_4 + H_2 \qquad \Delta H_r = 416\ \text{kJ/mol} \quad (6)$$

Assuming an inlet temperature of 25 °C and a 45% of conversion of octane to olefins (reaction 6), eq 5 was solved for the fraction of octane ($f_{burned}$) needed to be combusted to provide the heat of reaction 6. Results indicate that 6.25 mol % of the octane feed needs to be combusted to provide enough heat for autothermal operation of reaction 6. Assuming complete combustion of the octane according to reaction 7, the mole fraction of oxygen needed (if fed totally at the reactor inlet) for sufficient heat production for autothermal operation was calculated to be 45 mol %.

$$C_8H_{18} + 12.5O_2 \rightarrow 8CO_2 + 9H_2O \qquad \Delta H_r = -5074\ \text{kJ/mol} \quad (7)$$

However, according to the explosion limits, this percentage of oxygen is not within the safe operating zone. Since safe operation necessitates maximum oxygen mole fractions of 20−30 mol %, we conclude that, in the case of cofeeding oxygen in one stage at the reactor inlet, it is impossible to operate autothermally. Autothermal operation, however, would be possible when using multiple oxygen feeds, where local oxygen mole fractions are kept low.

**3.2. Reactor.** To prevent coupling reactions in the reactor during the COC process, products must be rapidly removed from the reaction zone. Thus, high gas hourly space velocities should be utilized (ranging from 100,000 to 1,000,000 $h^{-1}$) to minimize the residence time inside the reactor.[22] The reactor selection is done according to the method of Krishna and Sie.[21]

Fixed bed reactors (FBR), fluidized bed reactors (FLBR), and catalytic membrane reactors (Figure 7) are conceptually potential reactor choices for oxidation reactions.[22] The significant advantage of the FLBR is the possibility of achieving an isothermal catalytic bed, thus avoiding the hot spots typical of FBRs. For autothermal operation at low residence time, the utilization of a FLBR leads to better selectivities compared to a FBR. For the oxidative dehydrogenation of propane, butane, and isobutane, the use of these reactors led to remarkable selectivities to olefins.[22] The high selectivities achieved with this reactor were explained by the total oxygen consumption close to the distributor, hence inhibiting the consecutive combustion of the olefins formed at the beginning of the catalytic bed.

In addition, in a FLBR it is possible to utilize a distributed oxygen inlet along the catalytic bed.[22] Oxygen differentiation, assuming moderate gas back-mixing conditions in the FLBR, maintains a gas composition outside the flammable region and ensures safe operation. Moreover, controlled oxygen distribution minimizes the extent of complete combustion reactions. Thus, it is decided to use multiple oxygen feeds along the fluidized bed.

The utilization of a catalytic membrane reactor, although conceptually promising, is not considered for this process due to the cost of ceramic membranes.

**3.3. Separation.** The separation order is determined using the method of Barnicki.[23] On the basis of this method, alternative separation routes were developed (Figure 7) and compared. Separation trains that would result in the most efficient separation were selected. Similar to SC, the reactor outlet has to be quenched directly after the reactor to prevent coupling reactions. After quenching, the process stream consists of six groups of components that need to be separated: heavy oil ($C_5$ products + quench oil), light olefins ($C_2-C_4$) and alkanes ($C_1-C_4$), unconverted feed, combustion products (CO, $CO_2$, $H_2O$), and byproduct $H_2$. The liquid-phase products i.e., unconverted feed, quench fluid (quench oil and $C_5$ products), and water, should be separated first to prevent the formation of solids at high-pressure and low-temperature conditions later in the separation process. For similar reasons, removal of $CO_2$ at early stages is favorable. Figure 9 presents a functional flow sheet of the process, with block A representing the first separation unit and block B the second separation unit. In block A, the quench oil, water, and unconverted feed are separated and recycled. Afterward, $CO_2$ and remaining water are removed. In block B, light olefins ($C_2-C_4$) and alkanes ($C_1-C_4$) as well as the byproduct $H_2$ and CO are separated.

**3.3.1. Separation Block A.** Figure 10 represents the separation units of block A. To increase efficiency of separation, the utilization of two distillation columns is favored over the phase separators. In the first distillation column, 100% of the quench oil and $C_5$ products, 94% of the water and 78% of the unconverted hexane are recovered in the bottom stream. The remaining products (22% of the unconverted hexane, 6% of the water, $C_1-C_4$ olefins and alkanes, $CO_2$, CO and $H_2$) are fully recovered in the top stream. In the decanter water is separated from the apolar hydrocarbons. The hydrocarbon stream leaving the decanter consists only of 0.7% of water. The hydrocarbons are then separated with the second distillation column. The hexane stream (99.9% recovery) is sent to the reactor, and both the quench oil and

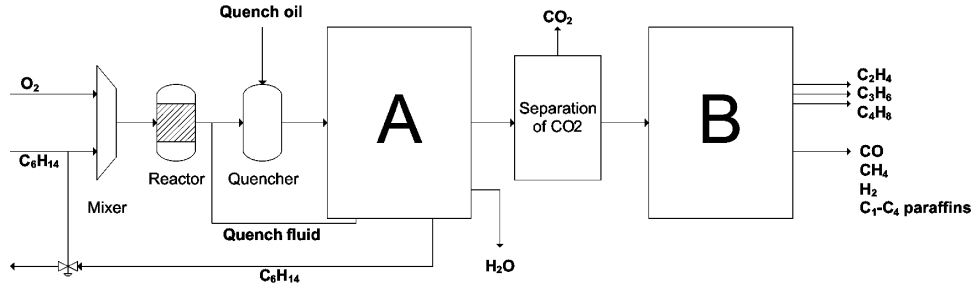


**Figure 9.** Functional flow sheet of the COC process.

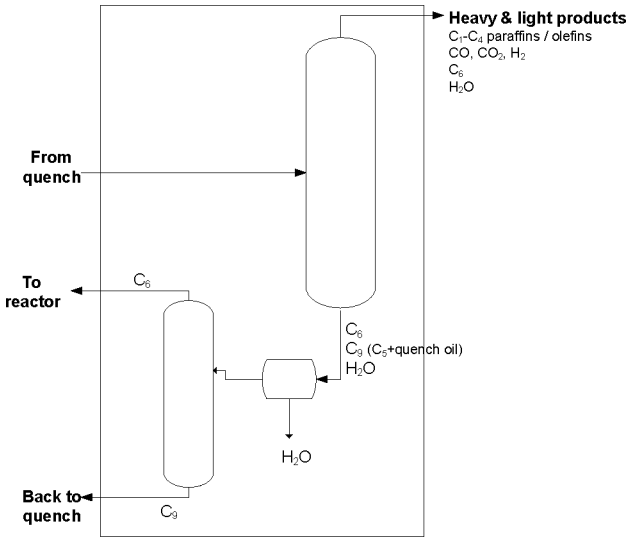


**Figure 10.** Separation units of block A.

$C_5$ products (modeled as nonane) (99.5% recovery) are sent to the quench.

**3.3.2. Sour Gas and Water Removal.** In practice, sour gases ($CO_2$, $H_2S$) are removed using absorption towers with amine solutions.[24] This technique is commercially available and is also used in this process design for $CO_2$ removal. The remaining 6% of water from the top stream of block A, together with water from the $CO_2$ absorption unit (amine−water solution), is separated by using a molecular sieve (MS 13X).

**3.3.3. Separation Block B.** Distillation columns are selected for the separation of all hydrocarbon streams. Compared to alternatives mentioned in Figure 7, e.g., absorption and PSA (99.5% recovery), distillation results in more efficient separation (99.99% recovery). The Olex process[25] can provide an efficient separation, as in distillation; however, this process requires a liquefied feed and hence is not considered as a suitable choice.

Because of the low relative volatility of $C_2/C_1$, $C_2/C_3$, $C_2/C_2^=$, and $C_3/C_3^=$, cryogenic distillation is needed for the separation of these products. Regarding the order of separation of the light products, i.e., $C_1-C_4$ olefins/alkanes, CO and $H_2$, it is decided, unlike in SC, to first separate the $C_4$ products from $C_3$ and all remaining lighter products ($C_2$, $C_1$, CO, $H_2$). $C_4/C_3$ separation is easier than $C_2/C_3$ separation and can be operated at low pressures. Pressurizing the stream after $C_4$ removal for $C_2/C_3$ separation will be less energy consuming. Figure 11 presents a block scheme for the separation block B. Butane and butylene are first separated from the process stream. Afterward, $C_2/C_3$ hydrocarbons are separated, followed by separation of $C_1/C_2$, $C_2^=/C_2$, and $C_3^=/C_3$. $H_2$ is recovered with a palladium−silver membrane, which is a method already used industrially.

## 4. Process Flow Diagram

For the simulation of the process, UNISIM Design Suite R380 is used. The property set chosen for the simulation is the Peng−Robinson equation of state. The process is designed for a total capacity of 300 kton/yr of $C_2^=-C_4^=$ products. Due to the lack of sufficient kinetic data, a simplified conversion model was used for the reactor, and simulation was performed starting from the reactor outlet. Hexane was used as a model compound of naphtha. For process simulation, a hexane-to-oxygen molar ratio of 5:3 was used. This amount of oxygen is not sufficient for autothermal operation but was selected for consistency with experimental conditions. The use of multiple oxygen feeds in the FLBR is expected to provide safe operation. A process overall hexane conversion of 45% was considered, and complete oxygen conversion was assumed. The reactor outlet composition was based on experimental results presented in Figure 3. Some of the separation units (e.g., sour gas removal) involve absorption and/or desorption processes and hence were not modeled. The distillation columns in block B were designed using the McCabe−Thiele method. Figure 12 presents a process flow diagram and a comprehensive mass balance of the COC process.

Fire and explosion index (F&EI) as well as HAZOP studies for COC indicate that the process has an intermediate degree of danger. Specifically, the risk of explosions demands extra safety precautions; therefore, extra pressure, temperature, and flow controls should be installed near the reactor. Extra safety valves are advisable near the reactor as well. The Chemical Exposure Index (CEI) indicates that, in terms of toxicity, the process is relatively safe, as there are no highly toxic chemicals in the process. Of course, this is no permit to neglect general safety procedures regarding toxic chemicals. With the extra safety measures, this plant is safe enough to be built.

## 5. Differential Study of Catalytic Oxidative Cracking vs Steam Cracking

The potential industrial application of the COC process depends on both the technical and economic advantages the process is able to achieve, as compared to the conventional SC process. Thus, to evaluate the COC process, a comparative study of both COC and SC processes is essential. The key process differences between the two processes are the following: (i) the presence of the catalyst in the COC; (ii) the feed−COC uses $O_2$ in the feed with no diluent while SC uses steam as diluent, (iii) the temperature of operation−SC operates at 800 °C while COC operates at 575 °C; (iii) SC uses an external source of heating, while in COC part of the heat of reaction is provided autothermally inside the reactor, thus reducing external fuel combustion; and (iv) the products formed lead to different separation orders in block B. These parameters introduce differences in the reactor design, product distribution, and separation trains; hence, there are significant differences in the

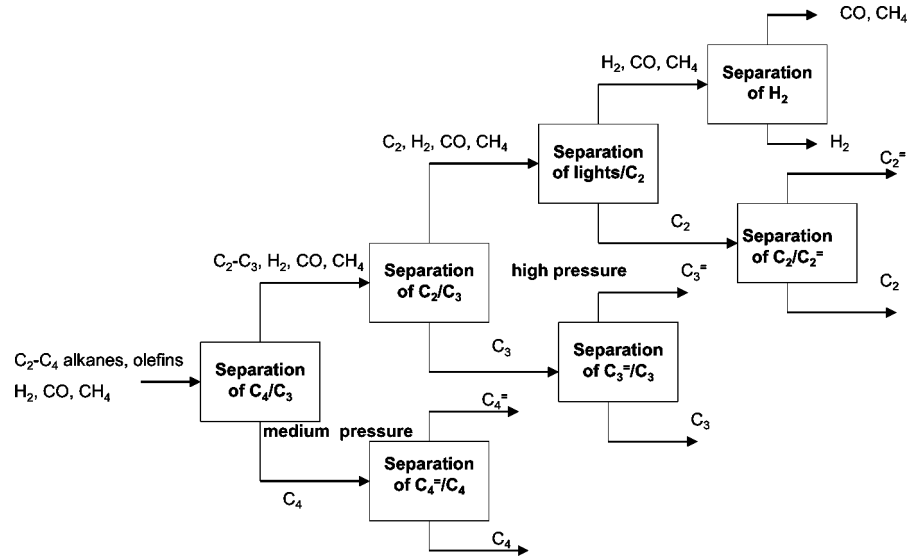


**Figure 11.** Block scheme for separation block B.

| | 1 | 2 | 3 | 4 | 5 | 6 | 7 | 8 | 9 | 10 | 11 | 12 | 13 | 14 | 15 |
|---|---|---|---|---|---|---|---|---|---|---|---|---|---|---|---|
| Temperature ( °C) | 20 | 20 | 71 | 300 | 348 | 76 | 60 | 0 | -144 | -14 | -7 | 36 | 44 | 69 | 130 |
| Pressure (kPa) | 100 | 100 | 100 | 100 | 101 | 100 | 1000 | 950 | 2950 | 2950 | 2950 | 1500 | 1500 | 950 | 950 |
| molar flow (Kmol/hr) | 1220 | 877 | 659 | 1540 | 4243 | 1553 | 2536 | 1912 | 625 | 339 | 83 | 417 | 20 | 161 | 249 |
| mole balance (Kmol/hr) | | | | | | | | | | | | | | | |
| n-hexane | 0 | 873 | 657 | 1530 | 842 | 657 | 185 | 185 | 0 | 0 | 0 | 0 | 0 | 0 | 185 |
| oxygen | 932 | 0 | 0 | 932 | 0 | 0 | 0 | 0 | 0 | 0 | 0 | 0 | 0 | 0 | 0 |
| hydrogen | 0 | 0 | 0 | 0 | 206 | 0 | 208 | 208 | 208 | 0 | 0 | 0 | 0 | 0 | 0 |
| water | 0 | 0 | 5 | 5 | 368 | 346 | 22 | 0 | 0 | 0 | 0 | 0 | 0 | 0 | 0 |
| CO | 0 | 0 | 0 | 0 | 304 | 0 | 304 | 304 | 304 | 0 | 0 | 0 | 0 | 0 | 0 |
| CO2 | 0 | 0 | 0 | 0 | 596 | 0 | 596 | 0 | 0 | 0 | 0 | 0 | 0 | 0 | 0 |
| Ethane | 0 | 0 | 0 | 0 | 29 | 0 | 29 | 29 | 0 | 0 | 29 | 0 | 0 | 0 | 0 |
| propane | 0 | 0 | 0 | 0 | 21 | 0 | 21 | 21 | 0 | 0 | 0 | 2 | 19 | 0 | 0 |
| n-butane | 0 | 0 | 0 | 0 | 64 | 0 | 64 | 64 | 0 | 0 | 0 | 0 | 0 | 0 | 64 |
| ethylene | 0 | 0 | 0 | 0 | 393 | 0 | 393 | 393 | 0 | 338 | 54 | 0 | 0 | 0 | 0 |
| propylene | 0 | 0 | 0 | 0 | 416 | 0 | 416 | 416 | 0 | 0 | 0 | 415 | 0 | 0 | 0 |
| 1-butylene | 0 | 0 | 0 | 0 | 161 | 0 | 161 | 161 | 0 | 0 | 0 | 0 | 0 | 161 | 0 |
| methane | 0 | 0 | 0 | 0 | 49 | 0 | 49 | 49 | 49 | 0 | 0 | 0 | 0 | 0 | 0 |
| nonane | 0 | 0 | 3.5 | 3.5 | 110 | 110 | 0 | 0 | 0 | 0 | 0 | 0 | 0 | 0 | 0 |
| Carbon and hydrogen balance closed within ±5% | | | | | | | | | | | | | | | |

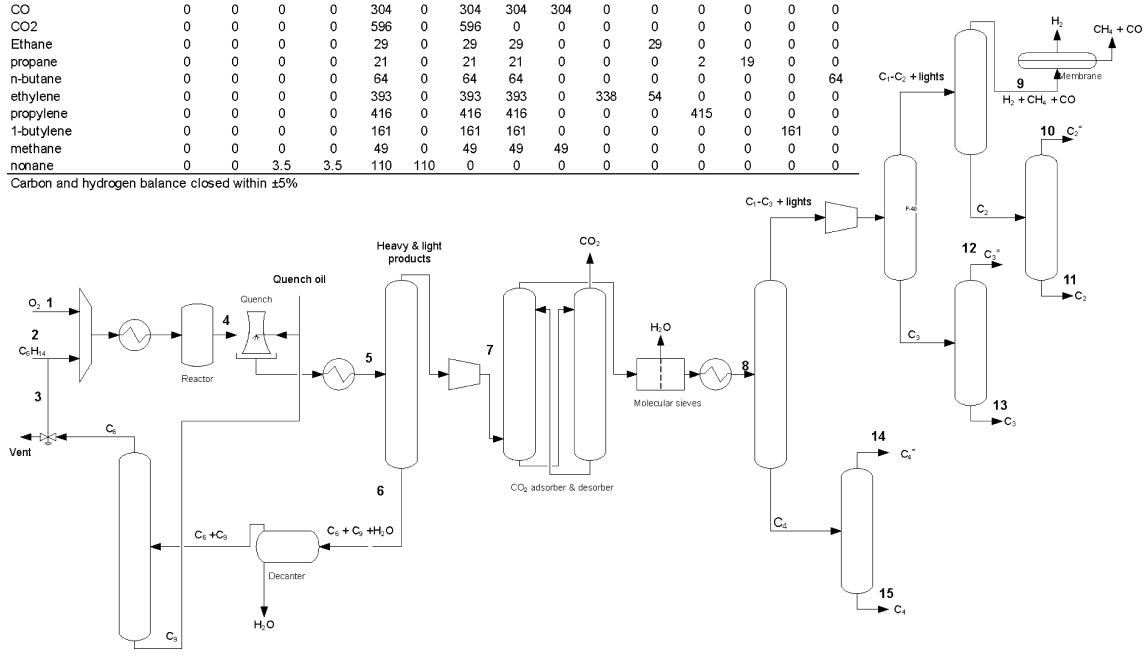


**Figure 12.** Process flow sheet of COC process and comprehensive mass balance.

energy consumption of the two processes. A functional block diagram of both processes is shown in Figure 13 and presents the key differences between these two processes.

The COC process, due to the presence of the catalyst and oxygen in the feed, operates at a much lower reaction temperature (575 °C) and results in a completely different product distribution than in SC. A simplified comparison of reactor outlet products of the COC of *n*-hexane (our results) and the SC of *n*-hexane at 720 °C[26] is shown in Table 2. The presence of the catalyst provides control over the olefin distribution, increasing the selectivity to total butylenes and propylene. COC results in a $(C_4^= + C_3^=)/C_2^=$ molar ratio of 1.5, against a $(C_4^= + C_3^=)/C_2^=$ molar ratio of 0.4 in SC. Previously, during the oxidative conversion of propane to propylene, Sinev and co-workers[27] reported that the abstraction of a secondary hydrogen atom from the alkane by surface $[O^-]$ sites ($[Li^+O^-]$ in Li/MgO) is energetically more favorable. Similarly, in the case of hexane, the high $(C_4^= + C_3^=)/C_2^=$ molar ratios are explained by the involvement of the catalyst in the process and the related preference for hydrogen abstraction from a secondary carbon atom, forming isohexyl radicals. $\beta$-Scission of isohexyl radicals at relatively mild cracking conditions ($T = 575$ °C) will result in a higher ratio of high olefins to ethylene. However, SC follows a radical chemistry route:[28] the carbon radicals (primary or secondary) formed initially via C−H bond cleavage, after

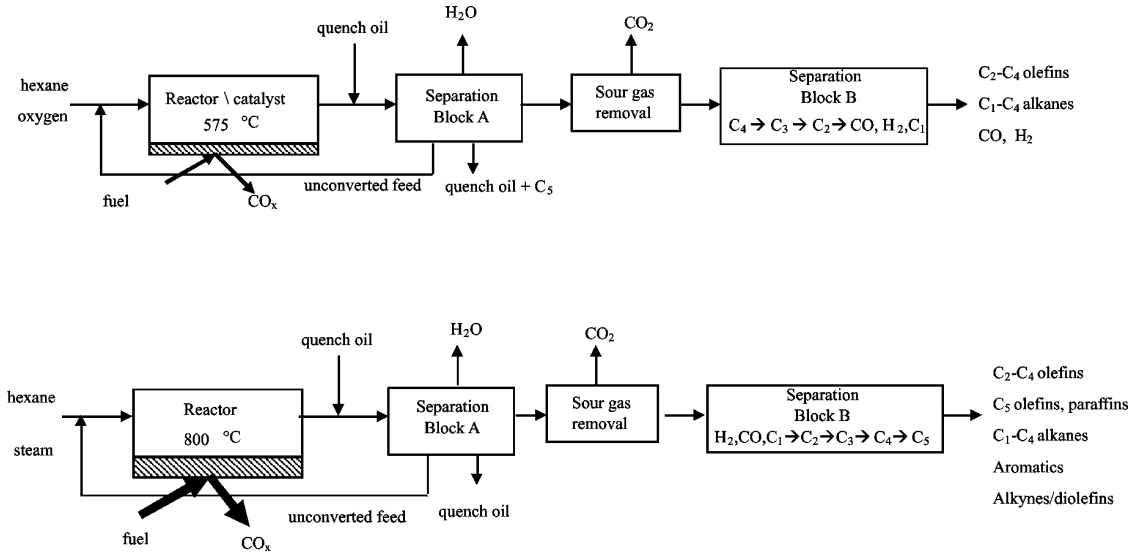


**Figure 13.** Key process differences between the COC and SC processes.

**Table 2. Reactor Outlet of Both COC and SC Processes**

| | mol/mol of hexane converted | |
|---|---|---|
| | COC | SC[26] |
| $H_2$ | 0.30 | 0.44 |
| CO | 0.44 | |
| $CO_2$ (from cracking reaction) | 0.87 | |
| $H_2O$ | 0.54 | |
| $C_1-C_4$ paraffins | 0.24 | 0.40 |
| $C_2^=$ | 0.57 | 1.33 |
| $C_3^=$ | 0.61 | 0.48 |
| $C_4^=$ | 0.27 | 0.02 |
| alkynes/diolefins | | 0.14 |
| naphthenes/aromatics | | 0.01 |
| other $C_5^+$ | 0.16 | 0.07 |
| $(C_4^= + C_3^=)/C_2^=$ | 1.54 | 0.38 |
| $CO_2$ from external fuel combustion[a] | 0.3 | 1.5 |

[a] Calculated $CO_2$ emission from methane combustion to provide sufficient heat to operate the reactor.

subsequent $\beta$-cleavage, result in primary radicals. Every further $\beta$-cleavage of the primary radicals formed results in $C_2$ product.

In the COC process, in addition to hydrocarbons, 1.3 mol of combustion products ($CO + CO_2$) per mole of hexane converted is formed. Carbon loss is hence considered a drawback of this process. In SC, however, byproducts like aromatics and diolefins have revenues. Total $CO_2$ emissions from the COC process (1.2 mol/mol of hexane converted) are slightly lower than emissions from SC (1.5 mol/mol of hexane converted).

The differences in product distribution in the two processes lead to differences in the separation trains. The separation of heavy products and quench oil (block A in Figure 13) in both processes is similar. In SC, however, there are more water and heavy components to be separated. In addition, in SC due to the higher reactor outlet temperature, approximately double the amount of quench oil is needed to cool the products. The composition of the light product stream, however, is very different in the two processes. Therefore, the separation order of the light product stream is fundamentally different (block B in Figure 13). The SC process is designed for a maximum ethylene production and recovery; hence, light olefins are separated first. The COC process is designed for production and recovery of propylene and butylene; hence, these olefins are separated first. In addition, a significant difference in the separation train of the two processes is the need for $CO_2$ separation in the COC process. Figure 14 presents a process flow sheet of the SC process obtained from the literature.[28]

The utilities (hot/cold) required for the COC and SC processes were estimated by performing heat integration of both processes. Heat integration was based on identifying both cold and hot streams and determining the pinch temperature.[18] Heat integration results of both COC and SC processes are presented in Table 3. Results indicate that the COC process consumes 53% less total duty than the SC process, making the process much more energy efficient. The high energy consumption in SC is mainly due to the large amount of hot utilities required for vaporization of water as diluent in the feed, as well as energy needed to heat the crackers to 800 °C. The COC process however, due to the lower operating temperatures, uses significantly less hot utilities, which makes the heat integration much more efficient than in SC (see Table 3). Heat integration of COC reduced the amount of utilities required for the process by 60%, while this was only 38% in SC. The specific amount of energy consumed in the SC process was calculated to be 17 GJ/ton of light olefins produced, while this was 8 GJ/ton of light olefins in the COC process. The claim that the COC process is more energy efficient is proven valid.

## 6. Economic Evaluation

We assume that the process design elaborated in the sections above for the COC of *n*-hexane is similar when naphtha is used as the feed. Hexane cracking has been used to model naphtha cracking in FCC processes, and results have been quite relevant with those of hexadecane in laboratory tests and the MAT tests in refineries.[19] On such a basis, the economic potential of the COC of naphtha was investigated.

The methods of Hill and Lang (±50% accuracy) were used to estimate the capital costs of the COC process.[29] The capital costs of the plant were estimated, utilizing equipment design and costs data (not shown here), to be $147 million. The operational costs consist of costs of feed stocks (naphtha and oxygen), utilities, maintenance and operations, depreciation (8% of total depreciable capital), and general expenses (12% of sales). Oxygen is purchased as a commodity chemical at a cost of $30/ton.[30] This price includes the cost of energy required for producing the oxygen. The pie diagram in Figure 15 presents the distribution of the operational costs. The total operational costs were estimated at $281 million per year, of which 74% is

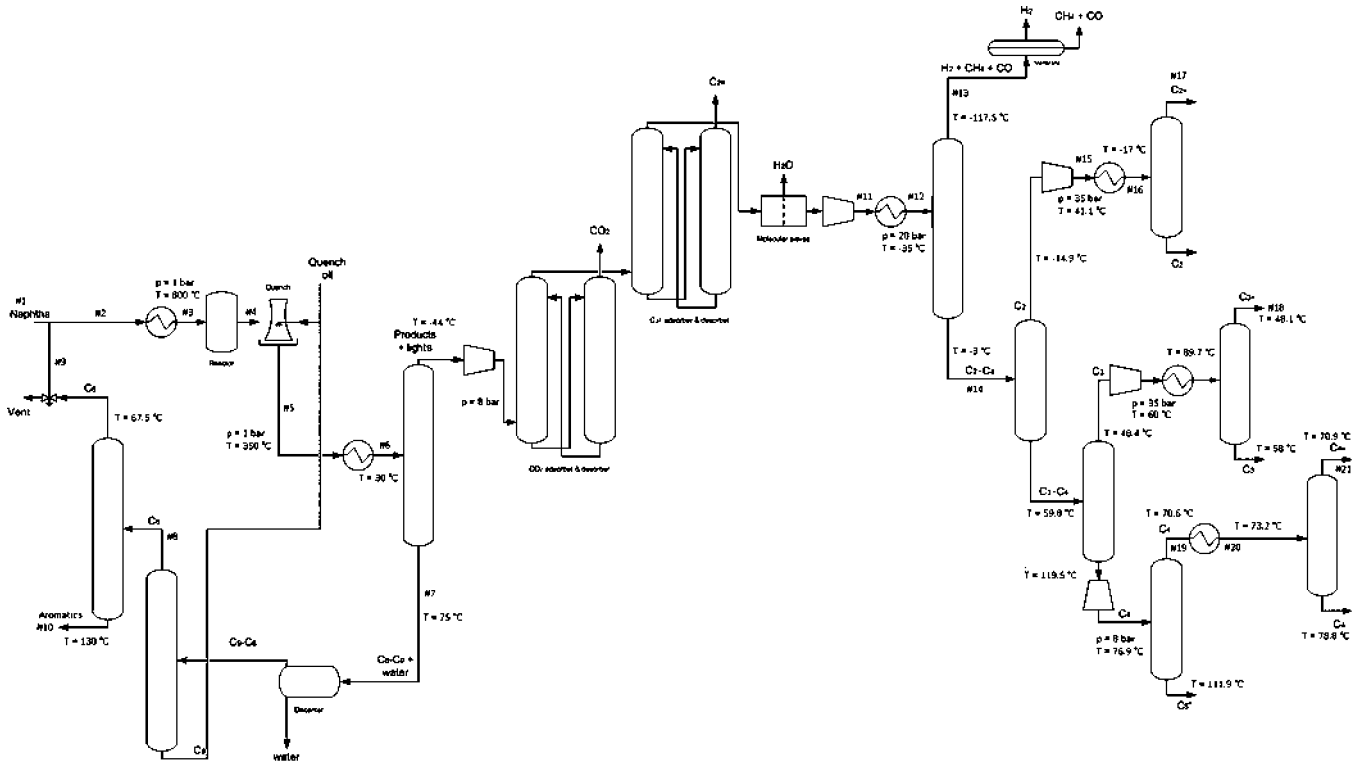


**Figure 14.** Process flow sheet of the steam cracking process.[28]

**Table 3. Hot and Cold Duties of the COC and SC Processes, before and after Heat Integration**

| | | SC | COC process |
|---|---|---|---|
| before heat integration | cold utilities (MW) | 107 | 121 |
| | hot utilities (MW) | 189 | 92 |
| | total duties (MW) | 296 | 213 |
| after heat integration | cold utilities (MW) | 50 | 57 |
| | hot utilities (MW) | 133 | 27 |
| | total duties (MW) | 183 | 85 |
| reduction by heat integration | | 38% | 60% |
| total duties compared to SC | | 100% | 47% |

the cost of naphtha feed. This implies that carbon loss as a result of combustion of part of the valuable naphtha feed makes the COC process economically less attractive than SC. In SC, methane (a cheaper fuel than naphtha) is utilized as fuel and naphtha feed is efficiently converted to products. Moreover, the heat utilities present only 3% of the total operational costs, which implies that the energy efficiency of the COC process as compared to SC does not result in significant savings in operational costs.

Using the current market prices in the Middle East of naphtha, ethylene, propylene, and butylenes,[31,32] the revenues of the COC process were estimated at $283 million per year. Thus, the insignificant difference between product revenues ($283M) and operation costs ($281M) strongly suggests that the COC process is economically yet unfeasible.

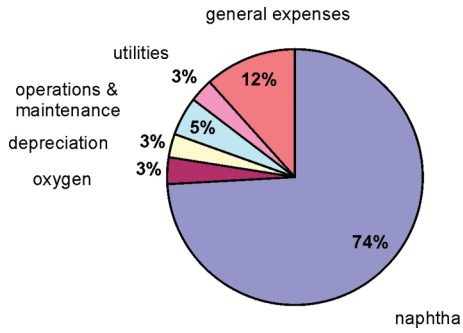


**Figure 15.** Pie diagram of operational costs.

**Table 4. NPV Analysis**[a]

| | scenario 1 | scenario 2 | scenario 3 | scenario 4 | scenario 5 |
|---|---|---|---|---|---|
| naphtha ($/kg)[b] | 0.5 | 0.5 | 0.6 | 1.0 | 0.8 |
| ethylene ($/kg)[b] | 1.0 | 1.0 | 1.0 | 1.5 | 1.0 |
| propylene ($/kg)[b] | 1.0 | 1.3 | 1.3 | 1.5 | 1.3 |
| butylene ($/kg)[c] | 0.8 | 1.0 | 1.0 | 1.0 | 1.0 |
| BEP (year) | | 4 | | | |
| NPV (mln USD) | −136 | 193 | −158 | −679 | −510 |

[a] It is assumed that the plant is built in year 0 and lifetime is 10 yrs. Discount rate of 10% is assumed. [b] Prices obtained from YNFX.[29] [c] Prices obtained from ICIS.[30] BEP, break-even point; NPV, net present value.

However, as it is predicted that in coming years the demand for propylene and butylene will increase, it is relevant to assume that the prices of these chemicals will also increase. Similarly, the demand for oil will probably increase as well, leading to an increase in the price of naphtha. Therefore, NPV analysis[18] for different scenarios was performed. The scenarios were defined as follows: *scenario 1*, current market prices were used; *scenario 2*, current market price of naphtha was used and 25% increase in the price of propylene and butylene was estimated; *scenario 3*, 25% increase in the price of each of propylene, butylene, and naphtha was estimated; *scenario 4*, prices as they were in 2008; *scenario 5*, average price of naphtha over the years 2008 and 2009 was used and 25% increase in price of propylene and butylene was estimated. Table 4 presents the NPV analysis of the five scenarios. It is clear from scenarios 4 and 5 that an increase in the price of naphtha has a detrimental effect on the NPV. The most promising scenario is scenario 2, with a $193 million profit at year 10. Scenario 5 would be, however, the most probable and realistic scenario. Nevertheless, even with

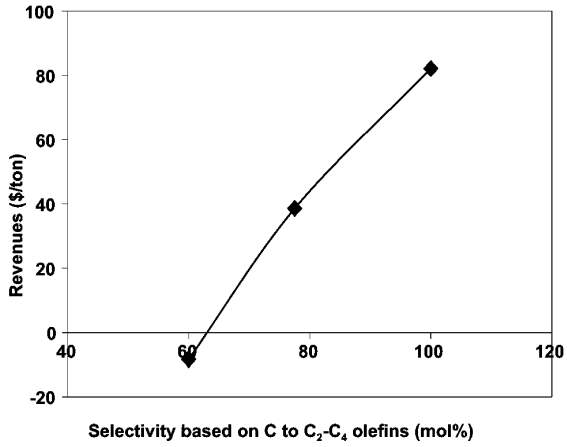


**Figure 16.** Revenues vs selectivity.

this scenario, the break-even point will not be reached after 10 years, and the loss after 10 years was estimated to be $510 million.

The performance of the Li/MgO catalyst and the selectivity to $C_2-C_4$ olefins are also influential factors in the economic feasibility of the COC process. Thus, a feasibility study was performed to see at which selectivity to olefins the process becomes economically attractive. Revenues were calculated for 100% conversion and a total $C_2-C_4$ olefin selectivity of 60%, 77.5%, and 100%. The current market prices and the relative fractions of the individual olefins, as reported in Figure 3, were used.

Figure 16 shows the revenues per ton of naphtha against the overall selectivity. Results indicate that the selectivity to $C_2-C_4$ olefins should be above 63 mol % for the COC process to break even. Thus we conclude that, based on the $C_2-C_4$ selectivities (63 mol %) achieved with the Li/MgO catalyst and the current market prices, the COC process will not be profitable. The profitability of the COC process is thus highly dependent on (i) the development of the market prices of ethylene, propylene, and butylene and (ii) the design of more selective catalysts with $C_2-C_4$ selectivities above 65 mol %. Catalysts that will enhance C−C bond cleavage in the alkane and further minimize combustion are essential.

In order to reduce the extent of combustion of the valuable naphtha feed and yet maintain an autothermal operation, recycling of $C_1-C_4$ paraffins and their combustion can be considered as a promising alternative.

Moreover, it is highly recommended to investigate reactor design parameters, specifically the catalyst volume-to-empty reactor volume ratio. Burch and Crabb[33] suggested that, during the oxidative conversion of propane, the combination of heterogeneous (catalytic) and homogeneous (gas-phase) reactions is necessary to obtain commercially acceptable yields of olefins. Similarly, in the case of oxidative cracking of naphtha, an optimized ratio of heterogeneous surface reactions to homogeneous gas-phase reactions is expected to significantly enhance the yields of olefins.

Finally, it is essential to realize that an experimental study using naphtha as the feed will provide more representative and accurate design data.

## 7. Conclusions

A conceptual design of the catalytic oxidative cracking process as an alternative to steam cracking for light olefins proved that the process is technically feasible. However, there are some constraints because the design is based on experimental data where reactants (hexane and oxygen) were diluted in helium. The presence of diluent in the process is economically not feasible; thus, pure hexane and oxygen have been considered as the feed. Safe operation, out of the explosion window, places severe restrictions on the feed composition. It is concluded that fully autothermal operation of the process is possible only with multiple oxygen feeds along the fluidized bed reactor.

In comparison to SC, the presence of the Li/MgO catalyst in the COC process (i) allows operation at 575 °C, which is much lower than temperatures utilized in SC, and (ii) controls the olefin distribution, increasing the ratio of $(\overline{C_4^=} + \overline{C_3^=})/\overline{C_2^=}$. The presence of oxygen is crucial to (i) internally provide heat for the endothermic cracking reaction, (ii) regenerate the catalyst, and (iii) inhibit coke formation.

The reactor products and separation train are very different for the two processes. The separation of the light hydrocarbon product stream proceeds in opposite order for the processes. The SC process is designed for maximum ethylene production and recovery, while the COC process is designed for production and recovery of propylene and butylene.

Energy evaluation of both processes clearly indicates that, compared to SC, the COC process is more energy efficient, with 53% less total duty use. However, utilities present only a minor fraction of the operational costs, which are controlled predominantly by the costs of the feedstock. Therefore, loss of valuable feedstock as a result of combustion of part of the naphtha feed makes the COC process economically less attractive than SC.

Finally, an economic evaluation of the COC process showed that, in a realistic scenario, this process is not yet economically attractive. For the process to be profitable, the market prices of propylene and butylene should rise about 25%. The design of more selective processes (optimized catalyst and reactor design) with selectivity to $C_2-C_4$ olefins above 65% should also be considered to increase the potential industrial applicability of the process.

## Acknowledgment

The authors thank ASPECT program, The Netherlands, for financial support (project no. 053.62.011). The authors also gratefully acknowledge the master students J. T. G. te Braake, R. M. van Dorp, Y. ter Mors, F. N. H. Schrama, and R. Veneman for performing this conceptual design, subsequent to their process design course at the University of Twente.

## Symbols

$f_{burned}$ = fraction of hydrocarbon burned [mol/mol]
$\Delta H_{combustion}$ = enthalpy of combustion [J/mol]
$\Delta H_{vap}$ = enthalpy of vaporization [J/mol]
HHV = higher heating value [J/mol]
$T_{boil}$ = boiling temperature [K]
$T_{reaction}$ = reaction temperature [K]
$C_{p,liquid}$ = specific heat capacity of the liquid [J/mol·K]
$C_{p,gas}$ = specific heat capacity of the gas [J/mol·K]
$\zeta$ = conversion [mol/mol]
$\Delta H_r$ = enthalpy of reaction [J/mol]

## Literature Cited

(1) Ren, T.; Patel, M.; Blok, K. Olefins from Conventional and Heavy Feedstock: Energy Use in Steam Cracking and Alternative Processes. *Energy* **2006**, *31*, 425–451.

(2) Cortelli, P. R.; Bakas, S. T.; Bentham, M. F.; Gregor, J. H.; Hamlin, C. R.; Smith, L. F. *Oleflex process—The proven route to olefins*; UOP: Des Plaines, IL, 1992.

(3) Bolt, H.; Zimmerman, H. In *Proceedings of the DGMK Conference*, Kassel, Nov 11−12, 1993 ; Baerns, M., Whitelamp, J., Eds.; Erdgas und Kohle e.V.: Hamburg, 1993; pp 175−183.

(4) Sarathy, P. R.; Suffridge, G. S. Etherify Field Butanes. *Hydrocarbon Process.* **1993**, *72*, 89–92.

(5) Ito, T.; Wang, J.-X.; Lin, C.-H.; Lunsford, J. H. J. Oxidative Dimerization of Methane. *J. Am. Chem. Soc.* **1985**, *107*, 5062–5068.

(6) Lin, C.-H.; Campbell, K. D.; Wang, J.-X.; Lunsford, J. H. Oxidative Dimerization of Methane over Lanthanum Oxide. *J. Phys. Chem.* **1986**, *90*, 4534–537.

(7) Morales, E.; Lunsford, J. H. Oxidative Dehydrogenation of Ethane over a Lithium-Promoted Magnesium Oxide Catalyst. *J. Catal.* **1989**, *118*, 255–265.

(8) Cavani, F.; Trifiro, F. The Oxidative Dehydrogenation of Ethane and Propane as an Alternative Way for the Production of Light Olefins. *Catal. Today* **1995**, *24*, 307–313.

(9) Xu, M.; Shi, C.; Yang, X.; Rosynek, M. P.; Lunsford, J. H. Effect of Carbon Dioxide on the Activation Energy for Methyl Radcial Generation over Li/MgO Catalysts. *J. Phys. Chem.* **1992**, *96* (15), 6395–6398.

(10) Landau, M. V.; Kaliya, M. L.; Gutman, A.; Kogan, L. O.; Herskowitz, M.; van den Oosterkamp, P. F. Oxidative Conversion of LPG to Olefins with Mixed Oxide Catalysts: Surface Chemistry and Reactions Network. *Stud. Surf. Sci. Catal.* **1997**, *110*, 315–326.

(11) Leveles, L.; Seshan, K.; Lercher, J. A.; Lefferts, L. Oxidative Conversion of Propane over Lithium-Promoted Magnesia Catalyst-II. Active Site Characterization and Hydrocarbon Activation. *J. Catal.* **2003**, *218*, 307–314.

(12) Leveles, L.; Seshan, K.; Lercher, J. A.; Lefferts, L. Oxidative Conversion of Propane over Lithium-Promoted Magnesia Catalyst-I. Kinetics and Mechanism. *J. Catal.* **2003**, *218*, 296–306.

(13) Trionfetti, C.; Babich, I. V.; Seshan, K.; Lefferts, L. Formation of High Surface Area Li/MgO-Efficient Catalyst for the Oxidative Dehydrogenation/Cracking of Propane. *Appl. Catal., A* **2006**, *310*, 105–113.

(14) Trionfetti, C.; Babich, I. V.; Seshan, K.; Lefferts, L. Presence of Lithium Ions in MgO Lattice: Surface Characterization by Infrared Spectroscopy and Reactivity Towards Oxidative Conversion of Propane. *Langmuir* **2008**, *24*, 8220–8228.

(15) Boyadjian, C.; Lefferts, L.; Seshan, K. Catalytic Oxidative Cracking of Hexane as a Route to Olefins. *Appl. Catal., A* **2010**, *372*, 167–174.

(16) Cavani, F.; Ballarini, N.; Cericola, A. Oxidative Dehydrogenation of Ethane and Propane: How Far from Commercial Implementation. *Catal. Today* **2007**, *127*, 113–131.

(17) van den Berg, H., *Process Plant Design course*; University of Twente: Enschede, The Netherlands, 2009.

(18) Seider, W. D.; Seader, J. D.; Lewin, D. R. *Product and Process Design Principles: Synthesis Analysis and Evaluation*, 2nd ed.; Wiley: New York, 2004; pp 243−396.

(19) Brait, A.; Koopmans, A.; Weinstabl, H.; Ecker, A.; Seshan, K.; Lercher, J. A. Hexadecane Conversion in the Evaluation of Commercial Fluid Catalytic Cracking Catalysts. *Ind. Eng. Chem. Res.* **1998**, *37*, 873–881.

(20) Bolk, J. W.; Westerterp, K. R. Influence of Hydrodynamics on the Upper Explosion Limit of Ethene-Air-Nitrogen Mixtures. *AIChE J.* **1999**, *45*, 124–144.

(21) Krishna, R.; Sie, S. T. Strategies for Multiphase Reactor Selection. *Chem. Eng. Sci.* **1994**, *49* (24, Part A), 4029–4065.

(22) Centi, G.; Cavani, F.; Trifiro, F. In *Selective Oxidation by Heterogeneous Catalysis*; Twigg, M. V., Spencer, M. S., Eds.; Fundamentals in Applied Catalysis *7*; Kluwer Acedemic: New York, 2001; pp 37−74.

(23) Barnicki, S. D.; Fair, J. R. Separation System Synthesis: A Knowledge-Based Approach 2. Gas/Vapour Mixtures. *Ind. Eng. Chem. Res.* **1992**, *31*, 1679–1694.

(24) Kohl, A. L.; Nielsen, R. B. *Gas Purification*, 5th ed; Gulf Publ.: Houston, TX, 1997; pp 148−181.

(25) Meyer, R. A. *Handbook of Petroleum Refining Processes*, 2nd ed.; McGraw-Hill:New York, 1997; pp 10.79−10.81.

(26) Le Van Mao, R.; Melancon, S.; Gauthier-Campbell, C.; Kletnieks, P. Selective Deep Catalytic Cracking Process of Petroleum Feedstocks for the Production of Light Olefins. *Catal. Lett.* **2001**, *73*, 181–186.

(27) Kondratenko, E. V.; Sinev, M. Yu. Effect of Nature and Surface Density of Oxygen Species on Product Distribution in the Oxidative Dehydrogenation of Propane over Oxide Catalysts. *Appl. Catal., A* **2007**, *325*, 353–361.

(28) Chauvel, A.; Lefebvre, G.; Marshall, N. *Petrochemical Processes: Synthesis-Gas Derivatives and Major Hydrocarbons*; Gulf Publ.: Houston, TX, 1989; pp 118−165.

(29) Peters, M. S.; Timmerhaus, K. D.; West, R. E. *Plant Design and Economics for Chemical Engineers*, 5th ed.; McGraw Hill: Boston, 2003; pp 226−278.

(30) Kirschner, M. J. Oxygen. *Ullmann's Encyclopedia of Industrial Chemistry*; Wiley-Interscience: New York, 2002.

(31) http://www.yarnsandfibers.com/textile-pricewatch (Accessed October 6, 2009).

(32) http://www.icis.com/staticpages (Accessed April 3, 2009).

(33) Burch, R.; Crabb, E. Homogeneous and Heterogeneous Contributions to the Oxidative Dehydrogenation of Propane on Oxide Catalysts. *Appl. Catal., A* **1993**, *100*, 111–130.

*Received for review* July 6, 2010
*Revised manuscript received* October 22, 2010
*Accepted* November 5, 2010

IE101432R